

A Vanadium Dioxide-PMMA Composite For Microwave Radiation Switching

Olesia I. Kucheriv,^[a] Valery I. Grygoruk,^[b] Viktor V. Oliynyk,^[b] Volodymyr V. Zagorodnii,^[b] Vilen L. Launets,^[b] Aurelian Rotaru,^[c] and Il'ya A. Gural'skiy*^[a]

- [a] O.I. Kucheriv, Dr. I.A. Gural'skiy
Department of Chemistry
Taras Shevchenko National University of Kyiv
64 Volodymyrska St., Kyiv 01601 (Ukraine)
E-mail: illia.guralskiy@univ.kiev.ua
- [b] Prof. V.I. Grygoruk, Dr. V.V. Oliynyk, Dr. V.V. Zagorodnii, Dr. V.L. Launets
Educational and Scientific Institute of High Technologies
Taras Shevchenko National University of Kyiv
64 Volodymyrska St., Kyiv 01601 (Ukraine)
- [c] Dr. A. Rotaru
Faculty of Electrical Engineering and Computer Science & Research Center MANSID
Stefan cel Mare University
13 Universitatii St., Suceava 720229 (Romania)

Supporting information for this article is given via a link at the end of the document.

Abstract: Reconfigurable radio-frequency components are highly demanded for modern communication systems as they can be involved in multiband and multistandard electronic devices. The key part of such components is an active switching element. In this work we offer a way to obtain an efficient microwave switch using vanadium dioxide–poly (methyl methacrylate) composite. Differential scanning calorimetry, SQUID magnetometry, and impedance spectroscopy measurements were used to characterize the phase transition in the proposed composite. Temperature induced metal-insulator transition occurs at technologically attractive 341 K. The transition leads to a change of microwave transmission trough VO₂-PMMA composite from -4.9 dB for low-temperature monoclinic form to -5.8 dB for high-temperature rutile form. This provides an ability to tune the material's transparency in the microwave range, while the shaping polymer matrix provides the proper mechanical processability of the switching element.

Introduction

Rapid development of wireless communication industry arise demands for reconfigurable components of devices which are suitable for signal routing, frequency switching, etc. Such components should be capable of tuning for a particular frequency band upon request. A good radio frequency (RF) switching component is supposed to allow the perfect signal transmission with no losses in the "on" state and to block energy transfer in the "off" state.^[1]

There are several kinds of technologies which are used nowadays for microwave radiation switching. They include switches based either on field effect transistors (FETs),^[2,3] PIN diodes,^[4,5] and MEMS^[6,7] elements or ferri- and ferromagnetic materials^[8,9] that are capable of the microwave energy flow control.

All these components have their own benefits and drawbacks. For example, FETs and PIN diodes are characterized by high operation speeds, low size and weight, but they can handle fairly low power.^[1] At the same time, MEMS provide perfect isolation

and insertion loss accompanied with relatively slow switching speed that makes them not suitable for applications where fast switching is needed.^[10] Additionally, the common disadvantage of MEMS switching elements is very expensive and time-consuming fabrication techniques, which results in high production cost.

In this context, different phase transition materials are gaining their popularity as prospective microwave switching elements. The working principle of these materials is based on the fact that different phase states of the same material can differently interact with a microwave radiation. Phase transition in such materials is usually triggered by the influence of temperature or electric current, which results in the change of some physical properties (e.g. electrical conductivity) and consequently, the material's ability to attenuate/transmit radiation of GHz frequency range.

For example, different chalcogenides like GeTe^[11] were shown to provide an efficient switching of radio frequency radiation.^[12] Additionally, our team recently showed an ability of coordination complexes, which undergo temperature induced spin crossover, to control GHz radiation upon the change of spin state.^[13–15] In this case microwave switching is realized due to the change of materials' permittivity during the spin transition. Also, there are several investigations of switchable interaction of microwave radiation with phase transition hybrid organic-inorganic perovskites.^[16,17]

Vanadium dioxide is one of the most studied and suitable for application among all phase transition materials offered for today.^[18] Since 1959, when phase transition in vanadium dioxide was discovered,^[19] it has attracted a wide attention of scientists working in the field of switchable materials. This compound displays a reversible metal-insulator transition (MIT) around technologically attractive temperature of 341 K and it is accompanied by a structural phase transition. In the low-temperature monoclinic phase with localized d-electrons, V–V dimers are formed. In the high-temperature rutile phase V⁴⁺ ions are aligned along the *c* axis with V–V distance of 2.88 Å. In this situation itinerant *d*-orbital electrons are shared among all vanadium ions resulting in the metallic nature of this material.^[20,21] This phase transition in VO₂ can be provoked by the change of

RESEARCH ARTICLE

temperature, application of electric or magnetic field, light irradiation, etc. In its turn, most of physical properties of VO₂ (such as optical absorption, electrical resistance, etc.) undergo significant changes as a result of MIT. This compound with outstanding switchable properties found its application for elaboration of thermochromic materials,^[22–25] actuators,^[26–28] photodetectors,^[29–31] field-effect transistors,^[32,33] memory devices,^[34] etc.

Among all possible applications, microwave radiation switching through phase transition in VO₂ attracts considerable attention. There were several reports on VO₂-based radio frequency switches, however most of them require technologically complicated and expensive techniques. For example, such switches are most commonly fabricated by pulsed laser deposition,^[12] RF sputtering,^[35] etc. A cheaper way to obtain VO₂-based radio-frequency switches by inkjet printing was offered in 2018 by Yang et al.,^[36] although this is rather specific technique. Meanwhile, development of polymer composites is a popular approach towards efficient microwave absorbers.^[37–43] In this paper we offer a new route towards low-cost VO₂-PMMA composite (PMMA = poly(methyl methacrylate)), which is suitable for microwave radiation switching and can potentially be integrated into a proper device.

Results and Discussion

VO₂-PMMA composite (**VO₂-PMMA**) was prepared by mechanical dispersion of VO₂ particles in PMMA solution with further evaporation of the solvent. In order to avoid the formation of cavities inside the composite, it was pressed in a steel press form under the presence of 8 MPa pressure and heated to softening point (120°C). The resulting content of VO₂ in the composite was 30% to avoid its brittleness while keeping good switchable response. Prior to composite preparation, VO₂ powder was grinded and the decrease of particles' size was controlled by scanning electron microscopy (Figure 1; grinded VO₂ powder (60 min) is further abbreviated as **VO₂^{pow}**). PXRD pattern of **VO₂^{pow}** is shown in Figure S1. Schematic illustration of process towards **VO₂-PMMA** is shown in the Figure S2.

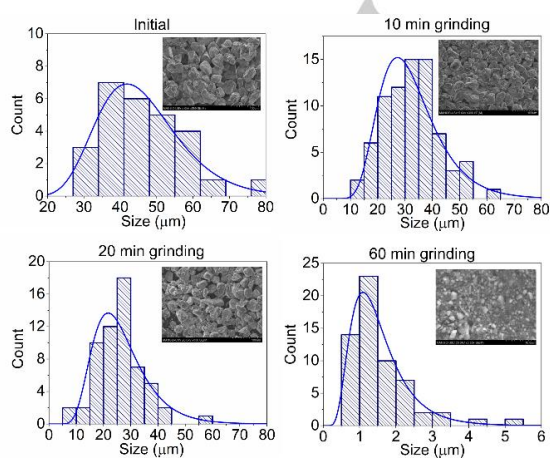


Figure 1. (a) SEM images of VO₂ particles and their size distribution plots, obtained after 10, 20 and 60 minutes of grinding.

Phase transition in the composite was monitored by differential scanning calorimetry in heating and cooling regimes (Figure 2a). In the heating mode MIT in **VO₂-PMMA** occurs at $T_{\uparrow} = 343$ K ($\Delta H = 3.2$ kJ mol⁻¹, $\Delta S = 9.3$ J mol⁻¹ K⁻¹ calculated per mol of VO₂), upon further cooling a transition back to the monoclinic phase is observed at $T_{\downarrow} = 331$ K ($\Delta H = 3.0$ kJ mol⁻¹, $\Delta S = 9.1$ J mol⁻¹ K⁻¹). Similar experiment was performed for **VO₂^{pow}** (Figure 2b). In the heating mode transition occurs at $T_{\uparrow} = 340$ K ($\Delta H_{\uparrow} = 9.0$ kJ mol⁻¹, $\Delta S_{\uparrow} = 26.5$ J mol⁻¹ K⁻¹), while upon cooling VO₂ transits back to the insulating state at $T_{\downarrow} = 332$ K ($\Delta H_{\downarrow} = 8.8$ kJ mol⁻¹, $\Delta S_{\downarrow} = 26.3$ J mol⁻¹ K⁻¹). One can see that the fabrication of polymer composite does not considerably affect the transition temperatures, the minor difference is associated with different thermalization of composite caused by the presence of polymer matrix. Additionally, the peaks in case of polymer composites are broadened. Phase transition in **VO₂-PMMA** was additionally characterized by SQUID magnetometry (Figure 1c), as MIT in VO₂ is accompanied by the change of magnetic susceptibility due to electronic and structural changes.^[44,45] According to the generally accepted theory, structural phase transition is responsible for the change from paramagnetic high-temperature phase with delocalized electrons of V⁴⁺ ions to non-magnetic low-temperature phase, in which two adjacent V⁴⁺ ions form dimers with simultaneous pairing of electrons ($S = 0$).^[46] This effect leads to the decrease of magnetic susceptibility upon transition from metallic to insulating state. The measurement showed the presence of temperature induced phase transition at $T_{\uparrow} = 340$ K and $T_{\downarrow} = 338$ K. The negative sign of $\chi_M T$ values originates from a contribution of the diamagnetic polymer. $\chi_M T$ vs. T plot for **VO₂^{pow}** is shown in Figure 1d, it displays phase transition behavior similar to **VO₂-PMMA**. Minor differences in transition temperature, observed in DSC and magnetic experiments, are associated with different sample thermalization.

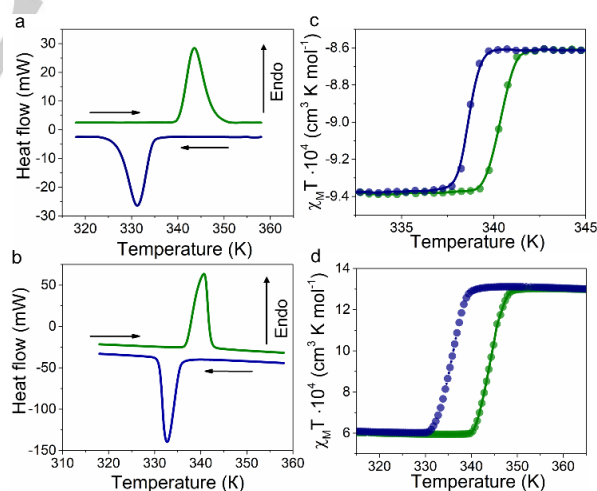


Figure 2. DSC measurements for **VO₂-PMMA** (a) and **VO₂^{pow}** (b), which demonstrate temperature induced phase transition. $\chi_M T$ vs. T plots for **VO₂-PMMA** (c) and **VO₂^{pow}** (d).

Using impedance spectroscopy measurements, we checked the ability of obtained composite material to change its ac conductivity upon heating (Figure 3). This technique was employed as an auxiliary way to characterize phase transition in the samples. The change of conductivity in the composite is very gradual given the

RESEARCH ARTICLE

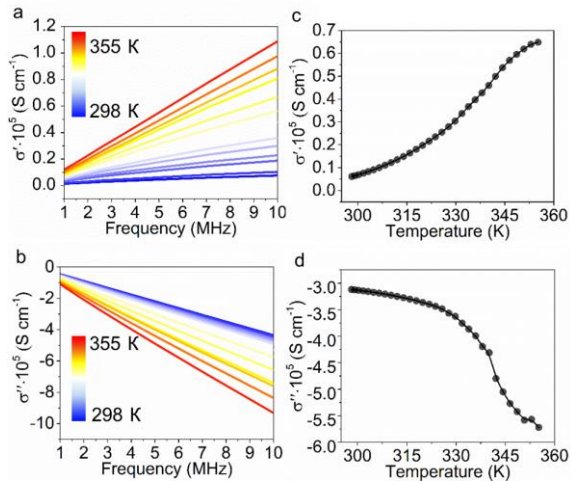


Figure 3. Real (a) and imaginary (b) parts of electric conductivity of $\text{VO}_2\text{-PMMA}$, measured at different temperatures in heating mode. σ' (c) and σ'' (d) vs. T plots at 7 MHz frequency, which display the change of conductivity, associated with MIT, despite the presence of polymer matrix excess, which separates VO_2 particles.

presence of non-conducting polymer matrix, therefore the values are determined at room temperature and temperature above transition: real part of conductivity of $\text{VO}_2\text{-PMMA}$ is $6.1 \cdot 10^{-7} \text{ S cm}^{-1}$ (7 MHz) at 298 K. Upon heating with the transition to metallic state, this value increases up to $6.5 \cdot 10^{-6} \text{ S cm}^{-1}$ (7 MHz) at 353 K. Additionally, the increase of σ'' is negative in the whole studied frequency range. σ'' value is $-3.1 \cdot 10^{-5} \text{ S cm}^{-1}$ (7 MHz) at 298 K and changes to $-5.7 \cdot 10^{-5} \text{ S cm}^{-1}$ (7 MHz) upon heating above MIT to 353 K. Negative values of σ'' cannot be explained by classical Drude model of electrical conductivity and may be indicative of carrier localization and/or backscattering. Similar behavior has been previously observed for VO_2 conductivity in THz range and was described by Drude-Smith model [47–49].

For comparison, impedance spectroscopy measurements were performed for pellets of VO_2^{pow} (Figure 4). In this case, the transition is much more abrupt and exact temperatures of MIT can be determined.

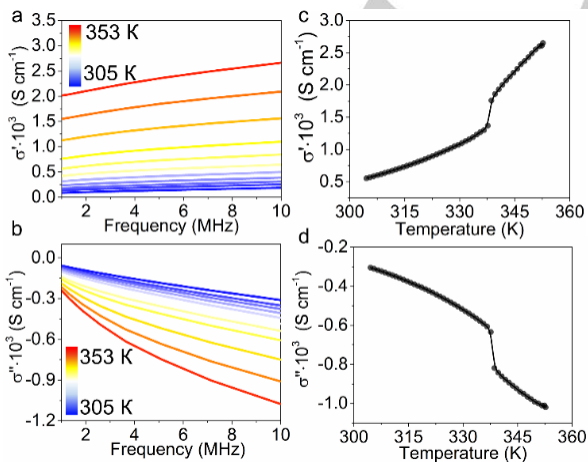


Figure 4. Real (a) and imaginary (b) parts of electric conductivity of VO_2^{pow} , measured at different temperatures in the heating mode. σ' (c) and σ'' (d) vs. T plots at 7 MHz frequency, which display the change of conductivity associated with MIT.

Thus, the starting value of σ' at 337 K (low-temperature-form) is 1.3 mS cm^{-1} (7 MHz) and it increases to 1.9 mS cm^{-1} (7 MHz) at 340 K due to MIT in the sample which is associated with structural changes that cause delocalization of electrons of V^{4+} ions. σ'' of VO_2^{pow} is found in the negative region similar to the polymer composite and changes from -0.6 mS cm^{-1} (7 MHz) at 337 K to -0.8 mS cm^{-1} (7 MHz) at 340 K (high-temperature form). Additionally, transition in VO_2^{pow} is more abrupt in comparison with $\text{VO}_2\text{-PMMA}$. Thus, the presence of polymer matrix significantly decreases the ac conductivity of VO_2 , although its variation upon MIT can still be detected.

Temperature dependent measurements of permittivity for $\text{VO}_2\text{-PMMA}$ and VO_2^{pow} obtained by impedance spectroscopy are given in Figure S3. At 298 K ϵ' and ϵ'' of $\text{VO}_2\text{-PMMA}$ are 79.5 and 1.5, respectively (at 7 MHz frequency). ϵ' and ϵ'' increase with the transition to metallic state and reach 145.0 and 16.3, respectively, at 353 K. The permittivity measurements of VO_2^{pow} revealed an interesting effect. The imaginary part of permittivity

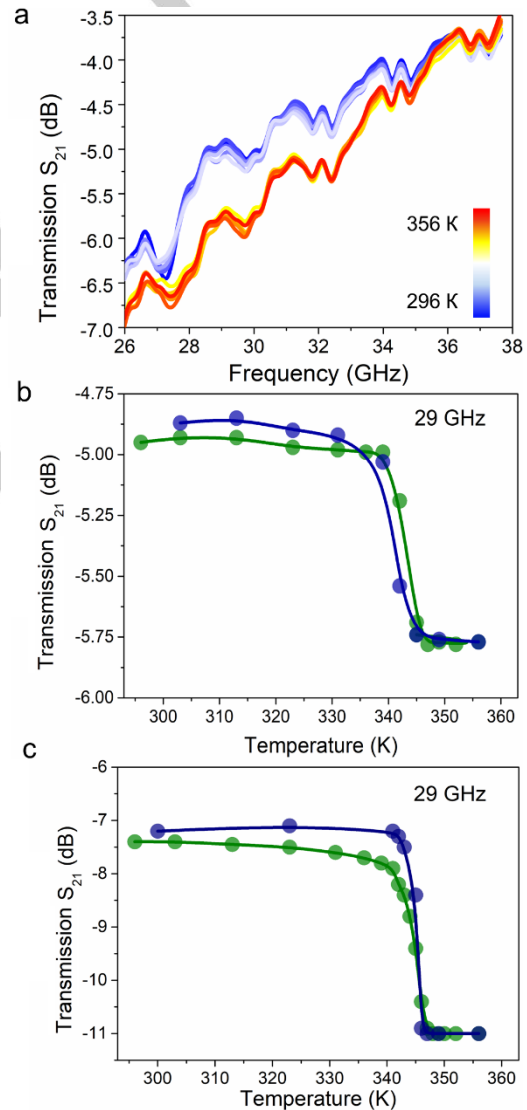


Figure 5. (a) Microwave transmission spectra of $\text{VO}_2\text{-PMMA}$ measured at different temperatures. (b) Transmission vs. temperature dependence, demonstrating a decrease as a result of MIT in $\text{VO}_2\text{-PMMA}$. (c) Transmission vs. temperature dependence, demonstrating a decrease as a result of MIT in VO_2^{pow} . The thickness of VO_2^{pow} was 2 mm.

RESEARCH ARTICLE

for this material is higher than the real part in both semiconducting and metallic states. ϵ' is 153 (7 MHz) at 337 K before the MIT, while ϵ'' is 328 at the same temperature. Additionally, ϵ'' exhibits a more significant increase during the transition to the metallic state: while ϵ' becomes 212.8 at 340 K (7 MHz), ϵ'' reaches the value of 468.4 at the same temperature. High values of the imaginary part of permittivity indicate the influence of VO_2^{pow} high electrical conductivity.^[50] Such effect is not observed for $\text{VO}_2\text{-PMMA}$ due to the presence of an insulating polymer matrix.

Temperature dependent measurements of microwave transmission were performed using scalar network analyzer in 26–38 GHz frequency range (Figure 5a). The thickness of studied $\text{VO}_2\text{-PMMA}$ was 750 μm . The most notable changes in microwave transmission upon MIT are observed in 27.5–35.0 GHz interval. For example, the transmission reaches -4.9 dB at 29 GHz and low temperature. An abrupt decrease of the transmission to -5.8 dB is observed upon heating with the transition to high temperature metallic state. At further cooling transmission changes back to its initial values (Figure 3b). The measurements for VO_2^{pow} were performed at fixed frequency of 29 GHz (Figure 5c). S_{21} is -7.2 dB at 341 K (just before the MIT). Microwave transmission through the sample abruptly decreases during transition to the metallic state and reaches -11.0 dB at 348 K. Even though the values of microwave transmission and its variation upon MIT are lower for $\text{VO}_2\text{-PMMA}$ given its smaller thickness and dilution with polymer, these observations confirm, that the presence of polymer matrix does not eliminate the ability of such composite to change the microwave attenuation during MIT inside the polymer matrix. Consequently, this facile way of fabrication can be successfully used for preparation of RF switches.

Complex permittivity of $\text{VO}_2\text{-PMMA}$ at variable temperature was additionally measured at fixed frequency of 29 GHz by the short-circuited waveguide method (Figure 6). When this measurement is performed, the end of a waveguide is terminated by the metallic plate, and all the incident electromagnetic energy is reflected that results in the formation of a standing wave.

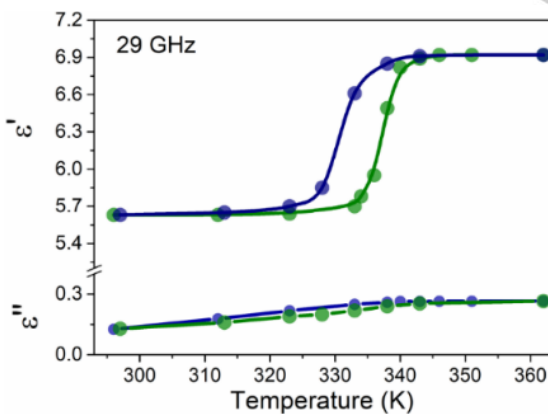


Figure 6. Temperature dependence of real and imaginary parts of permittivity in $\text{VO}_2\text{-PMMA}$ measured at frequency of 29 GHz, which demonstrates an increase, caused by MIT.

The material permittivity can be obtained by the standing wave parameters analysis. The reflection coefficient S_{11} , measured in

the short-circuited waveguide experiment (for non-ferri- or -ferromagnetic materials) can be expressed as follows:

$$S_{11} = \frac{\tanh \gamma d - \frac{\gamma}{\gamma_0}}{\tanh \gamma d + \frac{\gamma}{\gamma_0}} \quad (1)$$

where d is the sample thickness, γ_0 and γ are electromagnetic wave propagation constants in the empty waveguide and the sample-filled waveguide, respectively.

$$\gamma = \sqrt{k_c^2 - k^2}, \quad (2)$$

$$\gamma_0 = \sqrt{k_c^2 - k_0^2}, \quad (3)$$

where k_c is the critical wavenumber (defined by the waveguide mode and the waveguide cross-section); k and k_0 are the wavenumbers in the sample-filled waveguide and a free space, respectively.

$$k = \omega \sqrt{\epsilon_0 \epsilon \mu_0}, \quad (4)$$

$$k_0 = \omega \sqrt{\epsilon_0 \mu_0}, \quad (5)$$

where ϵ is the relative complex permittivity of studied material, ϵ_0 and μ_0 are permittivity and permeability of a free space, and ω is the angular frequency.

ϵ' of $\text{VO}_2\text{-PMMA}$ equals to 5.63 at room temperature and remains stable until reaching MIT temperature. Upon MIT, ϵ' increases up to 6.92. At the same time, ϵ'' increases just slightly from 0.13 at low temperature to 0.27 at high temperature.

Thus, thanks to the change of electrical properties in VO_2 during MIT, the obtained composite displays an ability to change microwave transmission in reconfigurable RF components; the polymer matrix enables easy shaping in fabrication. The most promising future application of the offered composite is an active component of reconfigurable antenna.

Conclusion

In this work we showed a novel approach towards fabrication of low-cost $\text{VO}_2\text{-PMMA}$ composites for microwave radiation switching. Preparation of polymer composites does not suppress the ability of vanadium dioxide to undergo metal-insulator phase transition. The obtained composite was shown to be effective microwave electromagnetic radiation switching upon temperature induced phase transition. The change of ac conductivity of $\text{VO}_2\text{-PMMA}$ upon MIT can still be detected despite the infill with the polymer matrix. Due to the facile way of fabrication the developed composite can be produced in any desired shape. As is easy to see, the switching ability of the composites can be also tuned by variation of VO_2 content and the switching element thickness, it was not the object of this work though.

Experimental Section

Materials

Vanadium dioxide and PMMA (average MW 550,000) were purchased from Abcr and used as received.

Preparation of $\text{VO}_2\text{-PMMA}$

Prior to composite preparation VO_2 powder was grinded for 60 minutes (controlled by SEM). 150 mg of PMMA was dissolved in 500 μl of chloroform. 75 mg of grinded VO_2 was dispersed in the obtained solution. Resulting mixture was sonicated during 15 minutes and transferred to the press form for air-drying. The obtained composite was pressed at 8 MPa,

RESEARCH ARTICLE

heated to the softening point of polymer (120 °C) and kept at this temperature for 15 minutes. The thickness of the resulting composite sample was 750 µm.

Characterization and measurements

PXRD patterns were acquired on Shimadzu XRD-6000 diffractometer using Cu-K α radiation (5–50° range, 0.05° step). Scanning Electron Microscopy (SEM) micrographs were recorded using a Hitachi SU-70 microscope. The particles have been deposited on an Al mount from a previously sonicated suspension in toluene. Differential scanning calorimetry (DSC) measurements were carried out using a PerkinElmer DSC 8500 operating at 20 K min⁻¹ for VO₂^{POW} and 100 K min⁻¹ for the VO₂-PMMA in the temperature range of 300–380 K. Different sweep rates were used in order to obtain relevant peak intensities for both samples, which have quite big difference in ΔH and ΔS values. ΔH and ΔS of composite are calculated excluding the polymer component. Microwave transmission measurements were performed using P2–65 scalar network analyser operating in Ka frequency band. The analyser was equipped with a hollow rectangular waveguide (7.20 mm × 3.40 mm). Heating was performed with an external thermostat. The sample of VO₂^{POW} was pressed in the waveguide by applying 20 MPa pressure (d = 2 mm). Electrical impedance measurements have been performed with a CONCEPT 40 Broadband Dielectric Spectrometer (Novocontrol GmbH). The spectra have been recorded with an Alpha-A high performance frequency analyzer (3 µHz...10 MHz) in the 20 °C – 80 °C temperature range. The temperature was changed in sweeping mode at 1 K min⁻¹. Magnetic measurements were performed in the temperature range 320–350 K using a MPMS3 SQUID magnetometer (Quantum Design Inc.) in DC mode under the magnetic field of 2000 Oe. Cooling and heating rates were 3 K min⁻¹.

Acknowledgements

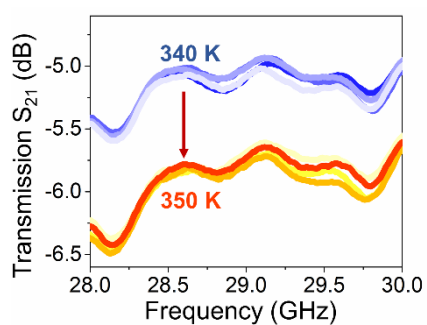
Authors acknowledge the financial support from the Ministry of Education and Science of Ukraine (grant DZ/112-2021). This work is dedicated to the people of Ukraine.

Keywords: microwave radiation switching • phase transitions • polymer composites • vanadium dioxide

- [1] R. H. Caverly, in *Wiley Encycl. Electr. Electron. Eng.*, John Wiley & Sons, Inc., Hoboken, NJ, USA, **1999**, pp. 199–234.
- [2] C. V. N. Rao, D. K. Ghodgaonkar, N. Sharma, *IEEE Microw. Wirel. Compon. Lett.* **2018**, *28*, 1128–1130.
- [3] D. P. Nguyen, A. Pham, F. Aryanfar, *IEEE Microw. Wirel. Compon. Lett.* **2016**, *26*, 696–698.
- [4] X. Zhang, X. Zou, C. W. Tang, K. M. Lau, *Phys. status solidi* **2017**, *214*, 1600817.
- [5] G. Upadhyay, V. S. Tripathi, *Microw. Opt. Technol. Lett.* **2017**, *59*, 1454–1460.
- [6] Y. Song, S. K. Ahn, M. Kim, J. Lee, C. Hwang, J. Pi, S. Ko, K. Choi, S. K. Park, J. Yoon, *Small* **2015**, *11*, 1390–1395.
- [7] S. Dey, S. K. Koul, *Microw. Opt. Technol. Lett.* **2016**, *58*, 1154–1159.
- [8] M. Vaseem, F. A. Ghaffar, M. F. Farooqui, A. Shamim, *Adv. Mater. Technol.* **2018**, *3*, 1700242.
- [9] A. Nafe, F. A. Ghaffar, M. F. Farooqui, A. Shamim, *IEEE Trans. Antennas Propag.* **2017**, *65*, 196–205.
- [10] I. Lysenko, A. Tkachenko, O. Ezhova, B. Konoplev, E. Ryndin, E. Sherova, *Electronics* **2020**, *9*, 207.
- [11] T. Singh, R. R. Mansour, in *2018 IEEE MTT-S Int. Microw. Work. Ser. Adv. Mater. Process. RF THz Appl.*, IEEE, **2018**, pp. 1–3.
- [12] P. Mahanta, M. Munna, R. Coutu, *Technologies* **2018**, *6*, 48.
- [13] O. I. Kucheriv, V. V. Oliynyk, V. V. Zagorodnii, V. L. Launets, I. A. Gural'skiy, *Sci. Rep.* **2016**, *6*, 38334.
- [14] O. I. Kucheriv, V. V. Oliynyk, V. V. Zagorodnii, V. L. Launets, O. V. Penkivska, I. O. Fritsky, I. A. Gural'skiy, *RSC Adv.* **2020**, *10*, 21621–21628.
- [15] O. I. Kucheriv, V. V. Oliynyk, V. V. Zagorodnii, V. L. Launets, I. O. Fritsky, I. A. Gural'skiy, in *Mod. Magn. Spintron. Mater.* (Eds.: A. Kaidatzis, S. Sidorenko, I. Vladymyrskiy, D. Niarchos), Springer Nature, **2020**, pp. 119–143.
- [16] A. Poglitsch, D. Weber, *J. Chem. Phys.* **1987**, *87*, 6373–6378.
- [17] H. Zangar, J. L. Miane, C. Courseille, N. B. Chanh, M. Couzi, Y. Mliik, *Phys. Status Solidi* **1989**, *115*, 107–118.
- [18] Y. Ke, S. Wang, G. Liu, M. Li, T. J. White, Y. Long, *Small* **2018**, *14*, 1–29.
- [19] F. J. Morin, *Phys. Rev. Lett.* **1959**, *3*, 34–36.
- [20] J. B. Goodenough, *Annu. Rev. Mater. Sci.* **1971**, *1*, 101–138.
- [21] C. Wu, F. Feng, Y. Xie, *Chem. Soc. Rev.* **2013**, *42*, 5157.
- [22] J. Zhang, H. Tian, L. Hao, X. Jin, C. Yang, J. Wang, X. Cui, C. Wang, C. Zhang, C. Zhang, Y. Xu, *J. Mater. Chem. C* **2016**, *4*, 5281–5288.
- [23] C. Ji, Z. Wu, L. Lu, X. Wu, J. Wang, X. Liu, H. Zhou, Z. Huang, J. Gou, Y. Jiang, *J. Mater. Chem. C* **2018**, *6*, 6502–6509.
- [24] F. Xu, X. Cao, H. Luo, P. Jin, *J. Mater. Chem. C* **2018**, *6*, 1903–1919.
- [25] Y. Ke, J. Chen, G. Lin, S. Wang, Y. Zhou, J. Yin, P. S. Lee, Y. Long, *Adv. Energy Mater.* **2019**, *9*, 1902066.
- [26] T. Wang, D. Torres, F. E. Fernández, A. J. Green, C. Wang, N. Sepúlveda, *ACS Nano* **2015**, *9*, 4371–4378.
- [27] H. Ma, J. Hou, X. Wang, J. Zhang, Z. Yuan, L. Xiao, Y. Wei, S. Fan, K. Jiang, K. Liu, *Nano Lett.* **2017**, *17*, 421–428.
- [28] K. Liu, C. Cheng, Z. Cheng, K. Wang, R. Ramesh, J. Wu, *Nano Lett.* **2012**, *12*, 6302–6308.
- [29] J. Zhou, M. Xie, H. Ji, A. Cui, Y. Ye, K. Jiang, L. Shang, J. Zhang, Z. Hu, J. Chu, *ACS Appl. Mater. Interfaces* **2020**, *12*, 18674–18682.
- [30] J. M. Wu, W. E. Chang, *ACS Appl. Mater. Interfaces* **2014**, *6*, 14286–14292.
- [31] K. T. Hong, C. W. Moon, J. M. Suh, T. H. Lee, S. Kim, S. Lee, H. W. Jang, *ACS Appl. Mater. Interfaces* **2019**, *11*, 11568–11578.
- [32] Y. Zhang, W. Xiong, W. Chen, X. Luo, X. Zhang, Y. Zheng, *Phys. Chem. Chem. Phys.* **2020**, *22*, 4685–4691.
- [33] M. Yamamoto, R. Nouchi, T. Kanki, A. N. Hattori, K. Watanabe, T. Taniguchi, K. Ueno, H. Tanaka, *ACS Appl. Mater. Interfaces* **2019**, *11*, 3224–3230.
- [34] T. Driscoll, H.-T. Kim, B.-G. Chae, B.-J. Kim, Y.-W. Lee, N. M. Jokerst, S. Palit, D. R. Smith, M. Di Ventra, D. N. Basov, *Science* **2009**, *325*, 1518–1521.
- [35] S. D. Ha, Y. Zhou, C. J. Fisher, S. Ramanathan, J. P. Treadway, *J. Appl. Phys.* **2013**, *113*, 184501.
- [36] S. Yang, M. Vaseem, A. Shamim, *Adv. Mater. Technol.* **2019**, *4*, 1800276.
- [37] L. L. Vovchenko, O. V. Lozitsky, L. Y. Matzui, V. V. Oliynyk, V. V. Zagorodnii, *Appl. Nanosci.* **2021**, 1–13.
- [38] L. L. Vovchenko, O. V. Lozitsky, V. V. Oliynyk, V. V. Zagorodnii, T. A. Len, L. Y. Matzui, Y. S. Milovanov, *Appl. Nanosci.* **2020**, *10*,

- 4781–4790.
- [39] O. V. Lozitsky, L. L. Vovchenko, L. Y. Matzui, V. V. Oliynyk, V. V. Zagorodnii, *Appl. Nanosci.* **2020**, *10*, 2759–2767.
- [40] G. Wang, Y. Wu, Y. Wei, X. Zhang, Y. Li, L.-D. Li, B. Wen, P.-G. Yin, L. Guo, M.-S. Cao, *ChemPlusChem* **2014**, *79*, 375–381.
- [41] S. He, C. Lu, G.-S. Wang, J. Wang, H.-Y. Guo, L. Guo, *ChemPlusChem* **2014**, *79*, 569–576.
- [42] A.-P. Guo, X. Zhang, S.-W. Wang, J.-Q. Zhu, L. Yang, G. Wang, *ChemPlusChem* **2016**, *81*, 1305–1311.
- [43] X. Luo, G.-S. Wang, H.-Y. Guo, X.-J. Zhang, W.-Q. Cao, Y.-Z. Wei, L. Guo, M.-S. Cao, *ChemPlusChem* **2014**, *79*, 1089–1095.
- [44] M. Liu, A. J. Sternbach, M. Wagner, T. V. Slusar, T. Kong, S. L. Bud'ko, S. Kittiwatanakul, M. M. Qazilbash, A. McLeod, Z. Fei, E. Abreu, J. Zhang, M. Goldflam, S. Dai, G.-X. Ni, J. Lu, H. A. Bechtel, M. C. Martin, M. B. Raschke, R. D. Averitt, S. A. Wolf, H.-T. Kim, P. C. Canfield, D. N. Basov, *Phys. Rev. B* **2015**, *91*, 245155.
- [45] C. Yin, R. Zhang, G. Qian, Q. Fu, C. Li, M. Wang, C. Zhu, L. Wang, S. Yuan, X. Zhao, H. Tao, *Appl. Phys. Lett.* **2017**, *110*, 172404.
- [46] R. Zhang, Q. S. Fu, C. Y. Yin, C. L. Li, X. H. Chen, G. Y. Qian, C. L. Lu, S. L. Yuan, X. J. Zhao, H. Z. Tao, *Sci. Rep.* **2018**, *8*, 17093.
- [47] N. Smith, *Phys. Rev. B* **2001**, *64*, 155106.
- [48] J.-H. Shin, K. Moon, E. S. Lee, I.-M. Lee, K. Hyun Park, *Nanotechnology* **2015**, *26*, 315203.
- [49] T. L. Cocker, L. V Titova, S. Fourmaux, H.-C. Bandulet, D. Brassard, J.-C. Kieffer, M. A. El Khakani, F. A. Hegmann, *Appl. Phys. Lett.* **2010**, *97*, 221905.
- [50] M. H. Khan, S. Pal, E. Bose, *Appl. Phys. A* **2015**, *118*, 907–912.

Entry for the Table of Contents



Here we describe a route towards microwave radiation switching using a composite material, which consists of vanadium dioxide and poly (methyl methacrylate) matrix. VO_2 displays a temperature induced metal-insulator phase transition which provides an ability to tune the material's transparency in the microwave range, while the presence of polymer matrix allows to give necessary shape to the switching element.